

ABEL INVERSION FOR DERIVING REFRACTIVITY PROFILE FROM DOWN LOOKING GPS RADIO OCCULTATION: SIMULATION ANALYSIS

A. MOUSA

National Research Institute of Astronomy and Geophysics, Helwan, Cairo, Egypt,
E-Mail : ashrafkm@yahoo.com

استنباط التوزيع الرأسى لمعامل الانكسار فى الغلاف الجوى باستخدام طريقة أبل العكسية وبيانات النظام العالمى للإحداثيات GPS
القادمة من أسفل والمستترة فى الغلاف الجوى

الخلاصة: تستخدم موجات ال GPS القادمة من أسفل والمستترة فى الغلاف الجوى فى حساب التوزيع الرأسى لمعامل الانكسار فى الغلاف الجوى. وتعتبر زاوية انحناء الأمواج كدالة فى معامل التأثر هي الأرصاد الرئيسية لهذا الاستخدام. توفر موجات ال GPS القادمة من أسفل كل من الأرصاد ذات زوايا الأرتفاع الموجبة والسالبة. ولحساب التوزيع الرأسى لمعامل الانكسار فى الغلاف الجوى يمكن استخدام طريقة أبل العكسية. وتطلب طريقة أبل شرط التماثل الكرى. و لذلك يتم حساب فرق زوايا انحناء الأمواج ذات زوايا الأرتفاع الموجبة و السالبة مما يعنى التخلص من تأثير طبقة الأيونوسفير. يقيم البحث الحالي طريقة أبل لحساب التوزيع الرأسى لمعامل الانكسار فى الغلاف الجوى باستخدام نماذج المحاكاة التى تستعين ببيانات النماذج الرياضية للغلاف الجوى و كذلك أرصاد البالونات. و قد تم عمل تحليل البيانات باعتبار الغلاف الجوى فى حالتيه الجافة و الرطبة. و قد أظهرت النتائج أنه يمكن استخدام طريقة أبل لحساب التوزيع الرأسى لمعامل الانكسار بدقة عالية. و كانت قيمة الخطأ النسبى المئوية فى حدود ٠,٢%.

ABSTRACT: Down Looking (DL) GPS radio occultation can produce an estimate of the atmospheric refractivity profile. The main observations are the bending angle as a function of the impact parameter. DL Provides both negative as well as positive elevation angle measurements. Abel inversion can be operated on a profile of partial bending angle found by subtracting the positive elevation measurement from the negative one with the same impact parameter. Abel inversion requires the spherical symmetrical assumption. Basically, partial bending calculation removes the ionospheric bending and hence it is possible to use a single frequency GPS receiver.

The current paper introduces a simulation data for the case of a receiver on Mountain top. The simulation uses model refractivity from MSISE-90 Model as well as radiosonde data. Random noises are added to the bending angle profile before inversion. The result shows that it is possible to produce accurate vertical refractivity profile below the receiver altitude. The calculation of the water vapor profile is also made using temperature profile information from the MSISE-90 Model as well as radiosonde. The relative errors in the retrieved refractivity profile are always less than 0.2%.

INTRODUCTION

When electromagnetic signal passes through the atmosphere, it is refracted. The magnitude of the refraction depends on the gradient of refractivity normal to the path, which depends on the gradients of density and water vapor. Thus measurements of refraction will contain information on the density (and hence temperature) and the water vapor along the path. The effect is more pronounced when the signal traverses a long atmospheric limb path. A series of such a path at different tangent heights yields measurements containing information on the vertical profile of refractivity (fig. 1). Refractivity can be converted to a profile of temperature and/or water vapor. At radio frequencies, it is not possible to make direct and accurate measurements of the refracted angle. However, if the transmitter and receiver are in relative motion, the refraction introduces a change in the Doppler shift of the received signal, and this can be related to the refracted angle [Eyre, 1994; Larsen et al, 2004].

There were early proposals for remote sensing of the earth's atmosphere using such "radio occultation" or "refractometry" techniques [Fishbach, 1965; Lusignan et al, 1969]. However, due to technical limitations, till recently they have only been applied successfully to studies of the planetary atmosphere [e.g. Kliore et al, 1965]. With the advent of Global Positioning System (GPS), together with the possibility of GPS receiver aboard a Low Earth Orbiter (LEO), it is now used for accurately sensing the earth's atmosphere.

The high accuracy of the radio occultation measurements using GPS at wavelengths 19 and 24 cm was demonstrated [Melbourne et al., 1994; Ware et al., 1996; Kursinski et al., 1996, 1997; Rocken et al, 1997; Feng and Herman, 1999; Schreiner et al., 1999]. First experiments in other frequency bands have been conducted in 1989-1998 years at wavelengths 2 and 32 cm as described by Yakovlev et al. [1995] and Yakovlev [1998].

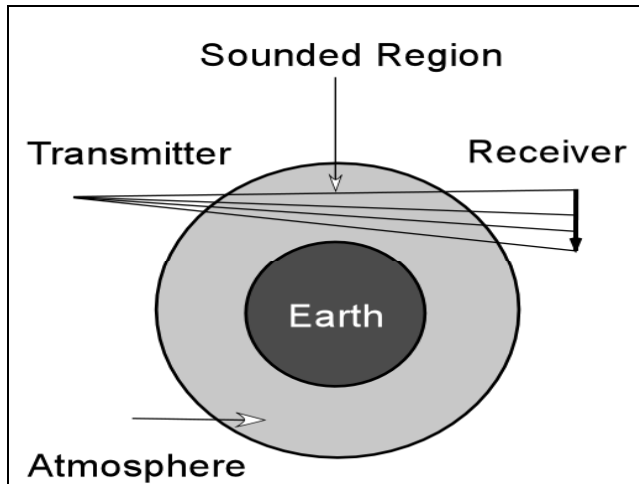


Fig. 1. Concept of refractivity profiling using Radio Occultation Technique

While GPS-LEO occultation data have the advantage of being global (One receiver in LEO provides about 500 globally distributed occultations per day), the sampling in any region is relatively sparse without a large number of orbiting receivers [e.g. Kursinski et al, 1997]. By contrast, a receiver located inside the earth's atmosphere (such as on a mountain top, or an airplane) can be used to provide data over specific areas of interest for the purpose of regional weather and climate studies [Cinzia et al, 1999].

A mountain-based or airborne receiver would track any GPS satellite as it sets or rises behind the earth's limb. Therefore data can be collected at both negative and positive elevation angles relative to the receiver local horizon (fig. 2). The Viewing geometry of a down-looking GPS receiver located inside the atmosphere can be considered as a hybrid between the space and the ground based geometry. It combines the high vertical profiling capabilities of space data (at least for heights below the receiver) with the benefit of routinely obtaining a relatively large number of daily profiles in region of interest. Every occultation will produce a profile of refractivity below the height of the receiver, with a diffraction-limited, vertical resolution of 150-250m.

One receiver with a full 360^0 field of view will observe nearly 96 occultations per day scattered within 200 km radius of the receiver. If the topography allows the use of several receivers, separated by distance of 50-200 km, hundreds of daily occultation can be obtained over that region. Such profiles when integrated with the accumulated water vapor distribution derived from ground based receivers, and possibly moisture information from any other accurate observations, is extremely useful for

regional weather monitoring as well as hydrological research.

For LEO occultation, Abel inversion is used to obtain the refractivity profile. Although fundamentally DL measurements are similar to the LEO measurements, it was originally thought that the limits of integration used in the Abel transform prevented its implementation when the receiver is inside the atmosphere [Zuffada et al. 1999]. In fact, it is possible to use an Abel inversion for the DL case. The measurement geometry is similar to the one considered by Bruton and Kattawar [1997] when inverting solar occultation data.

The current paper introduces down looking GPS occultation concept. The paper is organized as follows: section 2 introduces the GPS occultation technique and the Abel inversion to drive the refractivity profile from the observation. Section two ends with the procedure used to calculate the temperature and/ or vapor from the obtained refractivity. The simulation is carried out for a 3.8 km high Mountain. The simulation analysis and the results are introduced in section 3. The analysis indicates that GPS receiver inside the atmosphere can be used to retrieve accurately the refractivity profile with high resolution.

GPS OCCULTATION TECHNIQUE

For each occultation event, the GPS occultation data analysis chain from the measured phase delay to the derivation of the neutral atmospheric parameters and can be divided into three main steps [e.g. Mousa and Tsuda, 2001]:

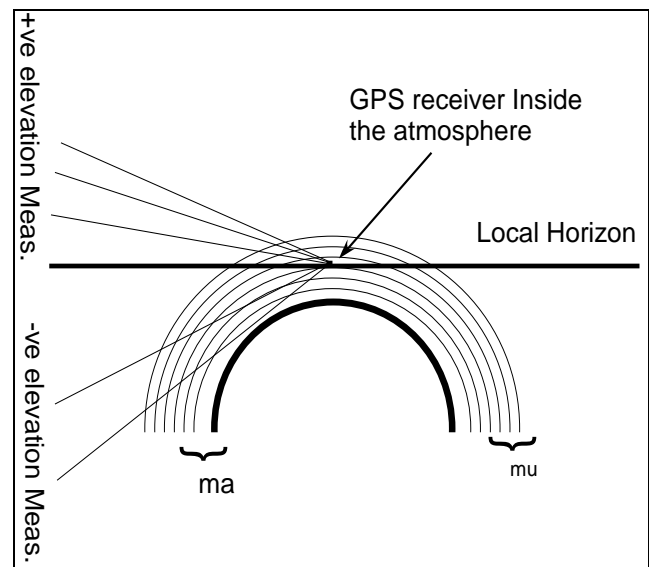


Fig. 2. A pictorial view of GPS down looking scheme. Atmospheric layers below the receiver

location are denoted by μ and those above the receiver by μ .

1. Calculation of the atmospheric bending angle profile from the observed L1/L2 excess phase path time series (L1 and L2 are the phases of the two GPS carrier frequency).
2. Retrieval of the refractivity profile from the atmospheric bending angle
3. Calculation of the density, pressure and temperature or water vapor profiles based on the retrieved refractivity profile.

BENDING ANGLE CALCULATION

In the geometric optics approximation, a ray passing through the atmosphere behaves according to Fermat's principle of least time. The ray travel along a curve defined by:

$$n \times r \sin(\varphi) = \text{constant} \equiv a \tag{1}$$

Where r is the distance from the origin of symmetry to a point on the ray path, φ is the angle between the direction of r and the tangent to the ray path, and n is the refractive index at r (fig. 3). Equation (1) corresponds to Snell's law in polar coordinates for a spherically symmetric medium, and known as Bouguer's formula. On this basis, a signal travelling in a spherically symmetric medium will bend by an angle (α) [Born and Wolf, 1980]:

$$\alpha = -2a \int_{a}^{\infty} \frac{1}{n \sqrt{(n^2 r^2 - a^2)}} \frac{dn}{dr} dr \tag{2}$$

Where a is the impact parameter of the ray.

The basic GPS data from which the bending angle (α) is derived are the L1 and L2 phase delay. From knowledge of the position of the transmitter (r_t) and the receiver (r_r) and their clocks (fig. 3), the extra delay due to the atmosphere can be isolated [e.g., Hajj et al., 1996].

From knowledge of the atmospheric extra delay as a function of time the extra atmospheric Doppler can be derived. This extra atmospheric Doppler is related to the bending of the signal via the equation:

$$\Delta f = -f/c \left(V_r^r \cos \Phi_r + V_r^\theta \sin \Phi_r + V_t^r \cos \Phi_t - V_t^\theta \sin \Phi_t \right) \tag{3}$$

Where f is the GPS transmitter frequency, c is the speed of light, V_r and V_t are the receiver and transmitter velocity vectors. The superscript r and θ indicate the radial and tangential component of the velocity vector, respectively. Φ_r and Φ_t are the angles between the ray bath and the direction of r as before, but for both the receiver and the transmitter respectively.

From equation (3) and the following equation, that is implied by Bouguer's formula,

$$r_t n_t \sin(\psi_t + \delta_t) = r_r n_r \sin(\psi_r + \delta_r) = a \tag{4}$$

(Angles are defined in figure 3) we can drive the total bending of the ray ($\alpha = \delta_t + \delta_r$) as a function of the impact parameter (a). This bending angle (α), as a function of the impact parameter (a), is the fundamental function to be inverted.

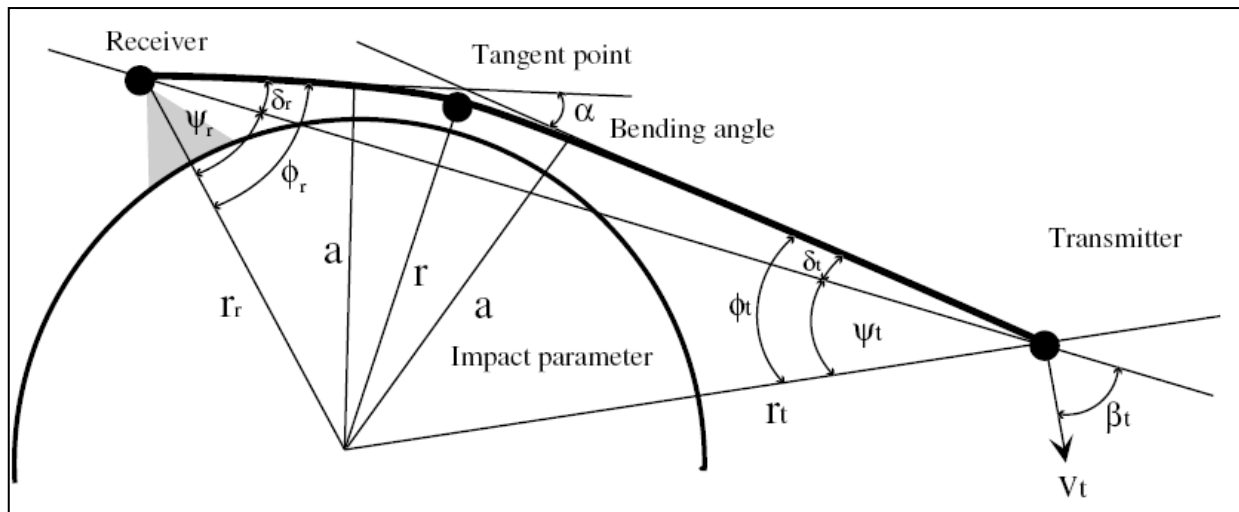


Fig.3. A schematic diagram defining the geometrical variables for a GPS transmitter/receiver link.

INVERSION SCHEME

The Abel inversion has been used extensively in seismic and astronomical inversions, as well as planetary and Earth occultation data [e.g. Fjeldbo et al. 1971; Kursinski et al. 1997]. Starting with the bending angle determined from the GPS Doppler shift, equation (2) is inverted with Abel inversion to give the refractive index [e.g. Tricomi, 1977]:

$$n(x) = \exp\left(\frac{1}{\pi} \int_a^\infty \frac{\alpha(a)}{\sqrt{(a^2 - x^2)}} da\right) \quad (5)$$

Where $x = nr$ is the refractive radius.

Unlike the LEO case, in DL occultations there may be significant ray bending along sections of the path above the receiver position, so the bending will not be equal on both sides of the tangent point. However Bruton and Kattawar [1997] noted that when the receiver is within the atmosphere, it is possible to observe rays at both positive and negative elevations. These refer to rays that intersect the receiver from above and below the local tangent. They also pointed out that, assuming spherical symmetry, for every negative elevation ray with bending angle α_{neg} there is a corresponding positive elevation value α_{p} with the same impact parameter value. Subtracting α_{p} from α_{neg} gives the partial bending angle α' (a)

$$\alpha'(a) = \alpha_{\text{neg}}(a) - \alpha_{\text{p}}(a), \quad (6)$$

Where α' (a) is the bending that occurs along the section of path below the receiver. By definition, as the tangent point approaches the receiver distance, r_r , the partial bending approaches zero.

The partial bending angle α' (a) can be written as:

$$\alpha'(a) = -2a \int_a^{n(r_r)r_r} \frac{d \ln(n)/dx}{\sqrt{(x^2 - a^2)}} dx \quad (7)$$

Where $x = nr$, $n(r_r)$ is the refractive index at the receiver position and r_r is the receiver position. Equation (7) can be inverted with,

$$n(x) = n(r_r) \exp\left(\frac{1}{\pi} \int_x^{x(r_r)} \frac{\alpha'(a)}{\sqrt{(a^2 - x^2)}} da\right) \quad (8)$$

Where $x(r_r)$ is the refractive radius at the receiver position.

CALCULATION OF ATMOSPHERIC PARAMETERS

In the third step of the data analysis, the atmospheric parameters density (ρ), pressure (P), temperature (T) and /or water vapor (e) are derived from the refractivity profile

using the dependence of refractivity on these parameters [e.g. Steiner et al., 1998]. Neutral refractivity (N) is given as [Smith and Weintraub, 1953]:

$$N = 77.6 P/T + 3.73 \times 10^5 e/T^2 \quad (9)$$

In regions where the atmosphere is drier than a volume-mixing ratio of 10^{-4} , the atmospheric parameters ρ , P, T can be derived directly from equation (9) (as the vapor pressure e is zero in that case). However, in a warmer tropical region, the contribution of the water vapor to refractivity is significant and cannot be ignored. In such a case, there is ambiguity between the temperature and water vapor. One can only solve for either the water vapor or the temperature using a priori meteorological and observation data.

An iteration process is proposed by Gorbunov and Sokolovskiy[1993] to solve for the water vapor, starting with temperature knowledge and assuming dry air and then derive the pressure using the hydrostatic equation. After that, the pressure and temperature is used (via equation (9)) to calculate a first estimate water vapor and so on. The procedure converges after two iterations.

SIMULATION ANALYSIS

In order to validate the algorithm's ability to retrieve refractivity (as well as temperature and /or water vapor) when a receiver is inside the atmosphere, we constructed three sets of simulated measurements; dry case, wet case and wet case based on Radiosonde observations. The receiver is fixed at 3.8 km altitude tracking GPS signals at both positive and negative elevations.

When the receiver is outside the atmosphere, bending measurements are smoothed over the time it takes the tangent height of the ray to descend the diameter of the first Fresnel zone [Kursinski et al., 1997]. In the geometric optics framework these smoothed measurements are approximately independent. Layer boundaries are then introduced between the tangent point of each of the measurements. The radius of the tangent point corresponding to a certain (α) measurement is estimated by solving the relation ($a = r \cdot n(r)$) where $n(r)$, the index of refraction at r , is obtained from the a priori model used as a first guess.

For a receiver inside the atmosphere, the bending measurements α_i are grouped into a set of m_a 'negative elevation' measurements and a set of m_p 'positive elevation' measurements. The typical behavior of the bending $\alpha(a)$ is given in figure (4). This figure shows that, for a fixed receiver, the transition between negative and positive elevation data correspond to the maximum (a) of the (α) vs. (a) curve. This property is used to separate the negative observation from the positive one.

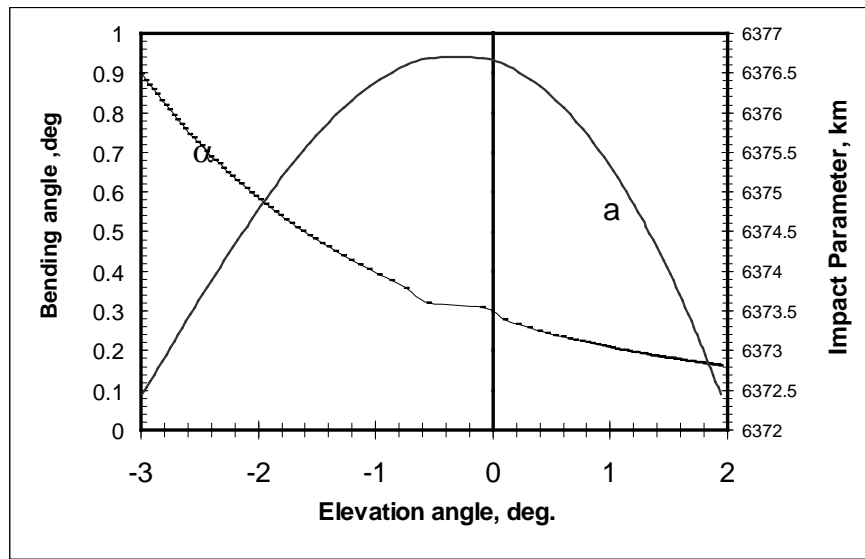
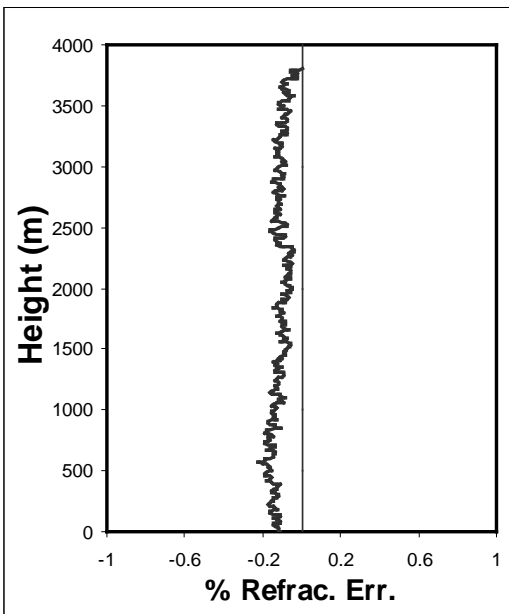
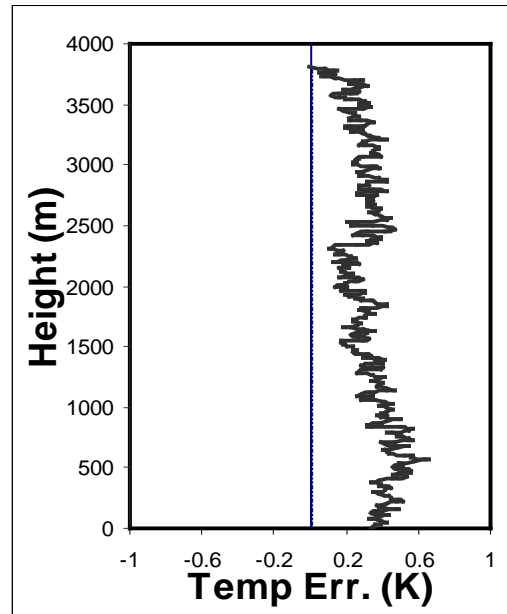


Fig. 4. bending (α) and impact parameter (a) as a function of elevation angle for a receiver at 3.8 km altitude.



a



b

Fig. 5. Dry atmospheric case. (a) Fractional error in retrieved refractivity as a function of height; (b) error in retrieved temperature as a function of height.

In all cases, starting with a model refractivity to be the truth, a set of rays linking the transmitter to the receiver were constructed with specified tangent heights, ranging from the earth's surface to the receiver's height. In a similar fashion, a set of rays linking the GPS satellite to the receiver was constructed to represent positive elevation angles above the receiver horizon. The positive measurements have impact parameter given by equation (1), where r is the radius of the receiver and ϕ is between 90° (0° elevation) and 180° (zenith). Noise was added to the simulated bending measurements assuming the standard deviation of the bending angle to be (σ) ($\sigma = 0.01 + 10^{-5}$ (radian)). This value accounts for the spherical approximation as well as to the receiver noise.

Dry case

The MSISE-90 [hedin, 1991] model is used here to represent the model refractivity from which the synthetic bending data were generated. The retrieved refractivity (after inversion) is compared to the model one to check the accuracy of the solution. The percentage of the fractional errors of the retrieved refractivity is introduced in figure (5-a). It is obvious from figure (5-a) that the errors are usually less than .2% up to the receiver height.

For this dry case, the temperature was driven using the hydrostatic equation following the procedure described before in section (2-3). From figure (5-b) we easily deduce that the error of the temperature retrieval is always less than 1 K. The temperature errors are gradually reduced from the earth's surface (about 0.6 K) to the receiver location (about 0.2 K).

WET CASE

Similar to the dry case, the MSISE-90 model is used here to represent the dry part of the model refractivity. The wet part is added by assuming water vapor pressure to follow an exponential model with scale height equal to 2.5 km. A weighting function is used to insure that the water vapor goes to zero at the height of 10 km. The total refractivity (dry + wet) is used as the model to derive synthetic bending data. The percentage of the fractional errors of the retrieved refractivity is shown in figure (6-a). Figure (6-a) shows that the errors are usually less than 0.2% up the receiver height.

For that wet case, water vapor was driven using the iterative procedure described earlier in section (2-3). The temperature is assumed known and taken from the MSISE-90 model. From figure (6-b) it is seen that the error of the water vapor retrieval is always less than 0.1 mbar.

RADIOSONDE BASED CASE

In this case the radiosonde observation is used to calculate the dry and wet refractivity model. The total refractivity (dry + wet) is used as the model to derive synthetic bending data. The percentage of the fractional errors of the retrieved refractivity is shown in figure (7-a). Figure (7-a) shows that the errors are usually less than 0.2%.

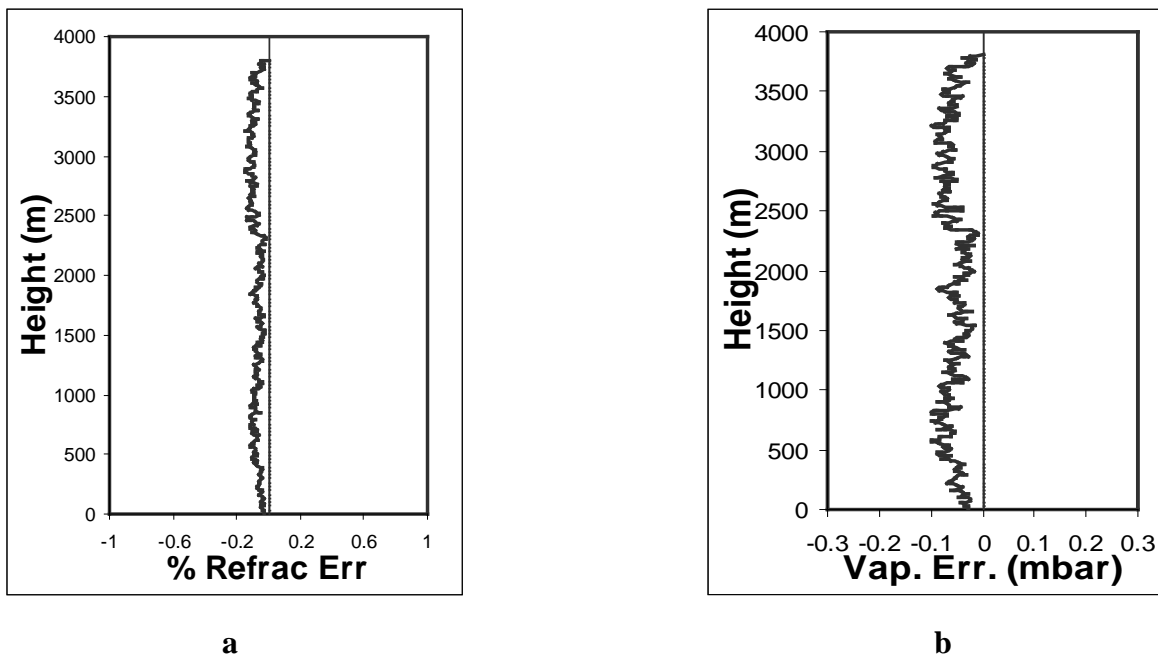


Fig. 6. Same as figure 5; but for the wet case. Both dry and wet part of the refractivity follow an exponential law; (b) water vapor retrieval errors.

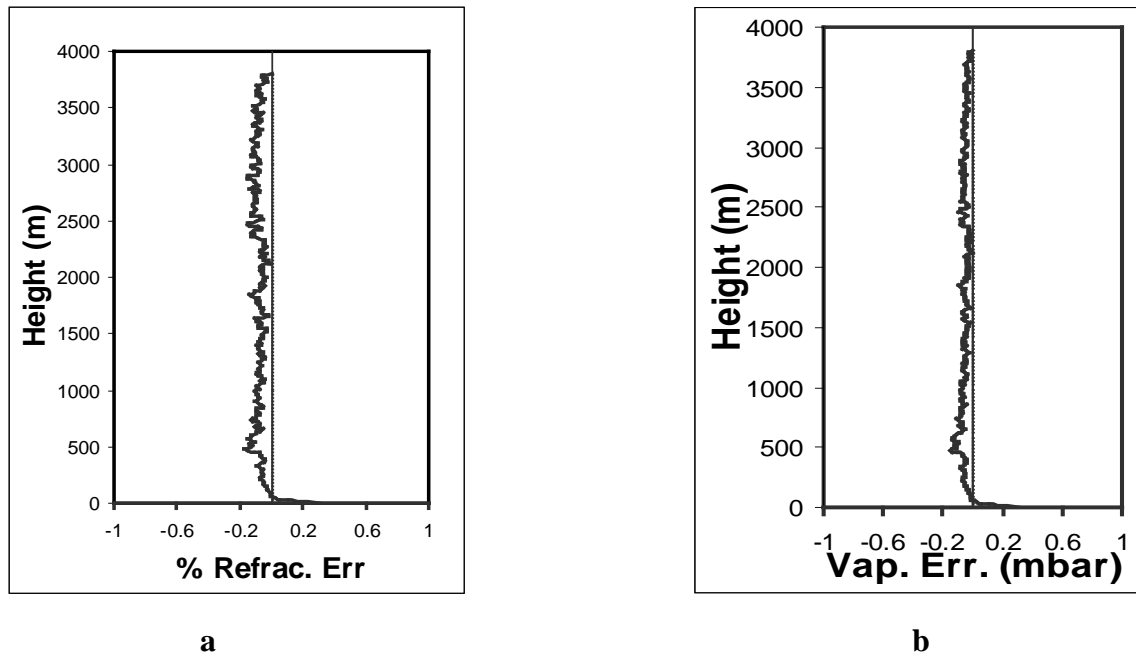


Fig. 7. Same as figure 6; but the wet part of the refractivity is driven from radio sonde data.

Water vapor again was driven using the iterative procedure described earlier in section (2-3). The temperature is assumed known and taken from the radiosonde observation. From figure (7-b) it is seen that the error of the water vapor retrieval is generally very small and always less than 0.1 mbar.

CONCLUSIONS

The paper describes and introduces the analysis of GPS occultation data for a receiver inside the atmosphere. The inversion technique can be used as a part of the data assimilation into numerical weather prediction system. The inversion technique is validated using data from MSISE-90 model as well as actual radiosonde observation. An exponential atmosphere was used for the validation, but the technique is general enough to be applied to any one dimensional atmospheric model.

Results of the simulation show that the bending angle measurements can retrieve the refractivity profile below the receiver altitude. The errors in the retrieved refractivity are always less than .2%. The results also show that, it is possible to derive the water vapor with errors less than .1 mbar. These results can improve the tropospheric models which in turn can help to improve the GPS position accuracy.

REFERENCES

- Born ,M., and E. Wolf. (1980)** "Principles of Optics", 6th ed., Pergamon, New York.
- Bruton W.D., G.W. Kattawar. (1997)** "Unique temperature profiles for the atmosphere below an observer from sunset images" *Appl. Opt* 36, 27, 6957-6961 pp.
- Cinzia, Z., G.A. Hajj, and E.R. Kursinski. (1999)** "A Novel approach to atmospheric profiling with a mountain-based or airborne GPS receiver" *J. Geophys., Res.*, 104, No. D20, 24435-24447 pp.
- Eyre, J.R. (1994)** "Assimilation of radio occultation measurements into a numerical weather prediction system" *Tech. Memo 199*, Eur. Cent. for Medium-Range Weather Forecasts, Reading, England.
- Feng, D.D., and B.M. Herman. (1999)** "Remotely Sensing the Earth's atmosphere using Global Positioning Syetem (GPS) – the GPS/MET data analysis" *J. Atmosphric and Oceanic Technology*, 16, 989-1002 pp.
- Fishbach, F.F. (1965)** "A satellite method for temperature and pressure below 24 km" *Bull. Amer. Meteorol. Soc.*, 9, 528-532 pp.

- Fjeldbo G, A.J. Kliore, V. Eshleman. (1971)** “The neutral atmosphere of venus studied with the mariner V radio occultation experiments” *Astron. J.*, 76, 2, 123-140 pp.
- Gorbunov, M.E., and S.V. Sokolovskiy. (1993)** “Remote sensing of refractivity from space for global observations of atmospheric parameters” rep. 119, Max-Planck-Institute for Meteorology, Hamburg.
- Hajj, G. A., E.R. Kursinski, W. I. Bertiger, S.S. Leroy, T. Meehan, L. J. Romans, and J.T. Schofield. (1996)** “Initial results of GPS-LEO occultation measurements of Earth’s atmosphere obtained with GPS/MET experiment” *Proc. Symp. On GPS Trends in Precise Terrestrial, Airborne, and Spaceborne Applications*, Springer-verlag, New York.
- Hedin, A.E. (1991)** “Extension of the MSIS Thermospheric Model into the Middle and Lower Atmosphere” *J. Geophys. Res.* 96, 1159-1991 pp.
- Kliore, A., D.L. Cain, G.S. Levy, V.R. Eshleman, G. Fjeldbo and F.D. Drake. (1965)** “Occultation experiment: results of the first direct measurement of Mars’ atmosphere and ionosphere” *Science*, 149, 1243-1248 pp.
- Kursinski, E.R., G.A. Hajj, W.I. Bertiger, S.S. Leroy, T.K. Meehan, L.J. Romans, J.T. Schofield, D.J. McCleese, W.G. Melbourne, C.L. Thornton, T.P. Yunck, J.R. Eyre, and N. Nagatani (1996)** “Initial results of radio occultation observations of Earth’s atmosphere using the Global Positioning System” *Science*, 271, 1107-1110 pp.
- Kursinski, E.R., G.A. Hajj, K.R. Hardy, J.T. Schofield, and R. Linfield. (1997)** “Observing Earth’s atmosphere with radio occultation measurement using the Global Positioning System” *J. Geophys., Res.*, 102, 23429-23465 pp.
- Larsen, G.B., K.B. Lauristen, F. Rubek and M.B. Sorensen. (2004)** “GRAS-SAF Radio Occultation Data from EPS/Metop” In *Occultations for Probing Atmosphere and Climate*, edited by G. Kirchengast, U. Foelsche and A. K. Steiner, pp 111-118, Springer, Germany.
- Lusignan, B., G. Modrell, A. Morrison, J. Pomalaza, and S.G. Ungar. (1969)** “Sensing the Earth’s atmosphere with occultation satellites” *Proc. IEEE*, 4, 458-467 pp.
- Melbourne, W.G., E.S. Davis, C.B. Duncan, G.A. Hajj, K.R. Hardy, E.R. Kursinski, T.K. Meehan, L.E. Young, and T.P. Yunck. (1994)** “The application of spaceborne GPS to atmospheric limb sounding and global change monitoring” *JPL Publication 94-18*, 147 pp., Jet Propulsion Lab, Pasadena, CA.
- Mousa, A.K., T. Tsuda. (2001)** “Retrieval of Key Climate Variables Using Occultation Geometry of a Mountain top GPS Receiver” *ION GPS 2001 proceedings*, 1117-1126 pp.
- Rocken, C., R. Anthes, M. Exner, D. Hunt, S. Sokolovskiy, R. Ware, M. Gorbunov, W. Schreiner, D. Feng, B., Herman, Y.-H. Kuo, and X. Zou. (1997)** “Analysis and validation of GPS/MET data in the neutral atmosphere” *J. Geophys., Res.*, 102, 29849-29866 pp.
- Schreiner, W.S., S.V. Sokolovskiy, C. Rocken, and D.C. Hunt. (1999)** “Analysis and validation of GPS/MET radio occultation data in the ionosphere” *Radio Sci.*, vol. 34, No. 4, 949-966 pp.
- Smith, E.K., and S. Weintraub. (1953)** “The constants in the equation for atmospheric refractive index at radio frequencies” *Proc. Of the I. R. E.*, 41, 1035-1037 pp.
- Steiner, A.K., G. Kirchengast, H.P., ladreiter. (1998)** “Inversion, error analysis, and validation of GPS/MET occultation data” *Ann. Geophysicae*, 17, 122-138 pp.
- Tricomi, F.G. (1977)** “Integral Equations” Dover, Mineola, New York.
- Ware, R., M. Exner, D. Feng, M. Gorbunov, K. Hardy, B. Herman, Y. Kuo, T. Meehan, W. Melbourne, C. Rocken, W. Schreiner, S. Sokolovskiy, F. Solheim, X. Zou, R. Anthes, S. Businger, and K. Trenberth. (1996)** “GPS sounding of the atmosphere from Low Earth Orbit: preliminary results” *Bull. Am. Meteorol. Soc.*, vol. 77, No 1, 19-40 pp.
- Yakovlev, O.I., S.S. Matyugov, and I.A. Vilkov. (1995)** “Attenuation and scintillation of radio waves in the Earth’s atmosphere from radio occultation experiments on satellite-to-satellite links” *Radio Sci.*, vol. 30, No. 3, 591-602 pp.
- Yakovlev, O.I. (1998)** “Space Radio Physics” Edited by Russian Fund of Fundamental Researches (RFBR), 478 PP., Moscow.